

Utilization of Magnetite Concentrate as an Additive in Adhering Fines of Quasi-particle and Its Effect on Assimilation Behavior

Ji-Won JEON,¹⁾ Sung-Wan KIM²⁾ and Sung-Mo JUNG^{1)*}

1) Graduate Institute of Ferrous Technology (GIFT), Pohang University of Science and Technology (POSTECH), Cheongam-ro 77, Pohang, 790-784 Korea. 2) Ironmaking Research Group, POSLAB, POSCO, Donghaean-ro 6261, Pohang, 790-300 Korea.

(Received on July 31, 2014; accepted on October 28, 2014)

In great efforts to utilize alternative iron ore resources in sintering process, it was attempted to use magnetite concentrate as an additive in adhering fines of quasi-particle and the effect of magnetite addition on assimilation behavior was investigated. A basic study was performed using the synthetic mixture of typical sinter composition with focus on the phase formation behavior of sinter. With small addition of magnetite, it was found that the formation of SFCA was increased with fixed CaO because Fe²⁺ probably replaced Ca²⁺ in the substitution mechanism of SFCA. Then the research was further extended by adopting quasi-particle concept using actual iron ores as a case study. Samples of coupled ore tablets simulating quasi-particle structure were prepared and experiments were carried out to investigate how magnetite addition affects the assimilation behavior of quasi-particle. Based on the experimental results and analysis, it was found that the small amount of magnetite addition, more specifically Fe²⁺ in magnetite, significantly influenced the physicochemical properties of melt as well as the structure of SFCA. The highest melt penetration depth was observed in N90-J10 sample containing 10 mass% magnetite ore J. As a result, it was concluded that the assimilation behavior was improved with proper amount of magnetite addition in adhering fines of quasi-particle.

KEY WORDS: magnetite concentrate; quasi-particle; assimilation; Silico-ferrite of calcium and aluminum.

1. Introduction

Blast furnace is still a major ironmaking process with its high energy efficiency and productivity. Since stable blast furnace (BF) operation requires the property control of raw materials, the sintering process is needed to convert fine iron ores into suitable lumpy agglomerates. The sinter ore is mainly composed of three main phases: iron oxides, calcium ferrites (which used to be called SFCA; Silico-Ferrite of Calcium and Aluminum) and silicates. Among the phases, SFCA is a desirable bonding phase and has been extensively studied on account of its important role in strength and reducibility. However, it has been found that SFCA has extremely complex nature with its variety of composition. Several researchers¹⁻⁵⁾ have studied the nature and composition range of SFCA. Inoue and Ikeda¹⁾ found the substitution plane of SFCA defined by the end members of CaO·3(Fe,Al)₂O₃–CaO·SiO₂. By reproducing Inoue and Ikeda's experiment, Mumme²⁾ found that SFCA is closely related to the aenigmatite group of minerals with the substitution plane, CaO·3(Fe,Al)₂O₃–2CaO·SiO₂·2(Fe,Al)₂O₃ of which end member is well fitted to the basic formula of aenigmatite X₂Y₆Z₆O₂₀ (where X=Ca²⁺, Na²⁺, K²⁺; Y=Ca²⁺, Mg²⁺, Fe²⁺, Fe³⁺, Al³⁺, Ti³⁺; Z=Fe³⁺, Al³⁺, Si⁴⁺). Several substitutions are available in aenigmatite-like

minerals and the possible substitution mechanism in basic iron ore sintering system (Fe₂O₃–Al₂O₃–CaO–SiO₂) can be described as follows:³⁻⁵⁾



Through this substitution, the end members of substitution plane for SFCA can be defined as CaO·3(Fe,Al)₂O₃–4CaO·3SiO₂. Furthermore, the substitution mechanism allows to estimate which elements contribute to form SFCA as well as in what proportions and under which conditions they react. The present study was motivated from the presence of Fe²⁺ in the above substitution mechanism which is expected to take place in SFCA formation reaction during sintering. Since SFCA is 'impure' calcium ferrite solid solutions with some substitutions of SiO₂ and Al₂O₃, the substitution reaction is essential for SFCA formation. If the presence of Fe²⁺ can make contribution to the substitution, it may affect the SFCA formation during sintering.

In the practical sintering process, the sinter mixture comprises several types of ores, fluxes, fuels and return sinter fines. Because the large variation of particle size is detrimental to the bed permeability, the mixture should be granulated to have a quasi-particle structure before charging onto the sinter strand. Due to the adhering of fine particles to the surface of large particles with added water, the coarser quasi-particle structure is beneficial to improve the sintering performance by enhancing bed permeability. Furthermore, to overcome the recent decline of resource circumstances,

* Corresponding author: E-mail: smjung@postech.ac.kr
DOI: <http://dx.doi.org/10.2355/isijinternational.55.513>

the design of effective quasi-particle structure by selective granulation was introduced and it was reported that the optimal design of quasi-particle would minimize the disadvantage of low quality ores.^{6–8)}

Figure 1 shows the schematic quasi-particle structure and procedure for the assimilation of quasi-particle. The quasi-particle consists of large nucleus particle in center and adhering fines of fine ores, flux and coke breeze. In the sintering process, the initial melt generates within adhering fines by forming calcium ferrites and silicates of low melting points. Then, the initial melt continues to react with the surrounding adhere particles and spreads out through the adhering layer to form the primary melt. Finally, the primary melt reacts with the nucleus and assimilation takes place. The ore property and sintering condition are important factors affecting the assimilation behavior of quasi-particle and the assimilative characteristics of each iron ore play an important role in controlling the reactions in the sintering bed as well as sinter qualities.^{9,10)}

The current study aims to perform fundamental research about the utilization of magnetite concentrates as an additive in adhering fines of quasi-particle. If the above hypothesis is verified, magnetite concentrates, more specifically, the Fe^{2+} in magnetite probably influence the structure of SFCA, which results in changing the physicochemical properties of melt as well as assimilation behavior of quasi-particle. The present investigation carried out two experiments. As a basic study, the first part clarified the effect of magnetite addition on phase formation behavior in the typical sinter composition by using analytical grade of chemical reagents. The second one, as a case study, investigated the effect of magnetite addition on assimilation behavior with coupled ore tablets simulating quasi-particle using actual iron ores.

2. Effect of Magnetite Addition on Phase Formation of Sinter

2.1. Materials Preparation and Experimental Procedure

Basic experiments were carried out to examine the effect of magnetite addition on sintering reaction using analytical grade of chemical reagents (particle size: under $1\ \mu\text{m}$). The phase formation behavior was investigated with three samples containing different levels of magnetite content in typical composition of sinter mixture. The chemical compositions of prepared samples are given in **Table 1**. Except for the mixing ratio of magnetite to hematite ($\text{Fe}_3\text{O}_4/\text{Fe}_2\text{O}_3$), all the samples have identical proportions of gangue level with the basicity ($\text{CaO}/\text{SiO}_2=1.8$), SiO_2 (6.7 mass%) and Al_2O_3 (1.3 mass%). Furthermore, total Fe content was maintained almost constant in the three samples (55.95 – 56.44 mass%) and the samples have been named according to the magnetite content. For example, there was no magnetite in Mag0, while 20 mass% of magnetite was added to Mag20.

To simulate the sintering condition, a confocal scanning laser microscope (CSLM) was employed. Disk-shaped samples (8 mm diameter \times 3 mm height) were prepared by pressing with 10 MPa, and then sintered at the simulated sintering temperature profile as shown in **Fig. 2**: RT to 800°C ($2^\circ\text{C}/\text{s}$) – holding at 800°C for 60 s – 800 to $1\ 300^\circ\text{C}$ ($20^\circ\text{C}/\text{s}$) – holding $1\ 300^\circ\text{C}$ for 120 s – $1\ 300$ to 400°C

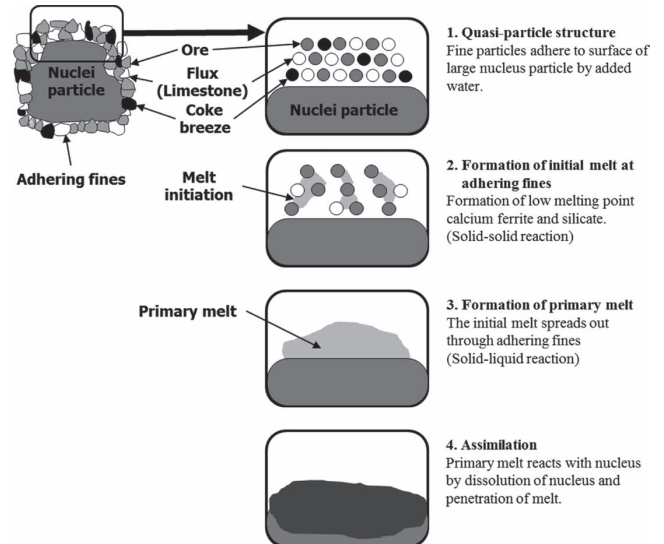


Fig. 1. Schematic drawing of quasi-particle structure and assimilation procedure.

Table 1. Chemical compositions of prepared sinter samples (mass%).

Sample	Fe_3O_4	Fe_2O_3	T.Fe	FeO	Al_2O_3	SiO_2	CaO	Basicity (CaO/SiO_2)
Mag0	0	80	55.95	0	1.3	6.7	12	1.8
Mag10	10	70	56.20	3.1	1.3	6.7	12	1.8
Mag20	20	60	56.44	6.2	1.3	6.7	12	1.8

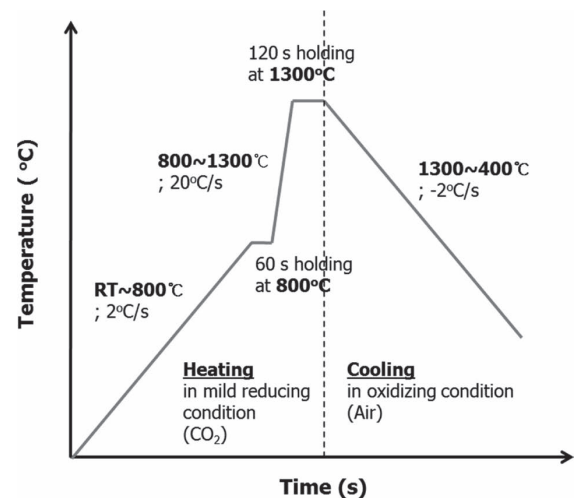


Fig. 2. Simulated sintering temperature profile used in the present work.¹¹⁾

($2^\circ\text{C}/\text{sec}$).¹¹⁾ Since the heating and cooling in actual sintering process are done by coke combustion and sucking air, respectively, heating was performed in CO_2 atmosphere and cooling was done in air.

2.2. In-situ Observation of Melt Formation

Since the phase formation behavior is closely related to the melt properties in the progress of sintering, in-situ observation of melt formation was carried out employing CSLM. **Figure 3** shows the in-situ observation results of melt formation behavior at $1\ 300^\circ\text{C}$. Larger volume of melt was observed in Mag0 sample containing no magnetite content while dispersed smaller volume of melt was identified

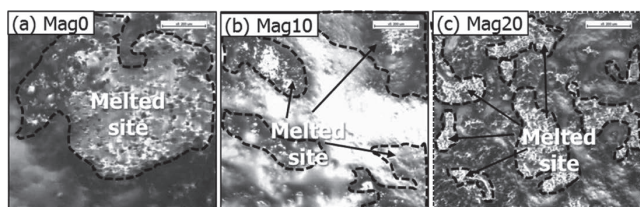


Fig. 3. In-situ observation results of melt formation behavior at 1300°C. The inside of the dotted line indicates the melted site.

in Mag20 sample containing 20 mass% of magnetite. The observation indicates that the addition of magnetite influences the melting behavior as well as melt property. The amount of melt was decreased and the viscosity of melt is believed to increase with increasing the magnetite content. There are some previous studies^{12,13)} which investigated the effect of magnetite on the melting behavior of sintering. They found that the magnetite is less reactive than hematite, that is, it is more difficult to generate melt with adding magnetite (Fe_3O_4) in sintering compared with hematite (Fe_2O_3). Further investigation was performed on the cross section of the samples to examine the effect of magnetite addition on phase formation using an optical microscope and electron probe micro analyzer (EPMA).

2.3. Microscopic Observation and Quantification of Phases

Figure 4 shows the optical microscopic observation results of the sintered samples where hematite, magnetite and SFCA were identified. In Mag0 sample (no magnetite addition), hematite and SFCA were the main observed phases. In Mag10 sample (10 mass% magnetite addition), some amount of magnetite phase was detected together with hematite and SFCA. However, the microstructure drastically changed in Mag20 sample (20 mass% magnetite addition) where relatively large amount of SFCA was seen in the entire sample area. On the other hand, the pore size was decreased compared to the other two samples. This is probably due to the increase of melt viscosity with increasing magnetite content, which limits the pore coalescence.

Since sinter microstructure has great inhomogeneity even in macroscopic observation, it is difficult to obtain the objective information of sinter sample. In this sense, EPMA sweeping area analysis might be very effective because this method targets the entire sample area.^{14,15)} The quantitative phase analysis result from EPMA sweeping area analysis is presented in Fig. 5. For the EPMA analysis, 15 kV and 50 nA beam was used and high purity standard materials of Fe_2O_3 (99.9 mass%), $CaSiO_3$ (99.9 mass%) and $CaAl_2O_5$ (99.9 mass%) were employed for calibration. In the current study, four main elements of SFCA, *i.e.*, Fe, Al, Si and Ca were analyzed with 200 points for each sample. The composition range of SFCA was assumed to be in between $2CaO \cdot Fe_2O_3$ (33 mol% of Fe_2O_3) and $CaO \cdot 3Fe_2O_3$ (75 mol% of Fe_2O_3) to classify the phases into iron oxides (above 75 mol% of Fe_2O_3) and silicate (below 33 mol% of Fe_2O_3) according to the Fe_2O_3 content in phase composition. From this result, it was found that the fraction of SFCA increased with increasing magnetite content while the fractions of iron oxides and silicates were decreased. From the above

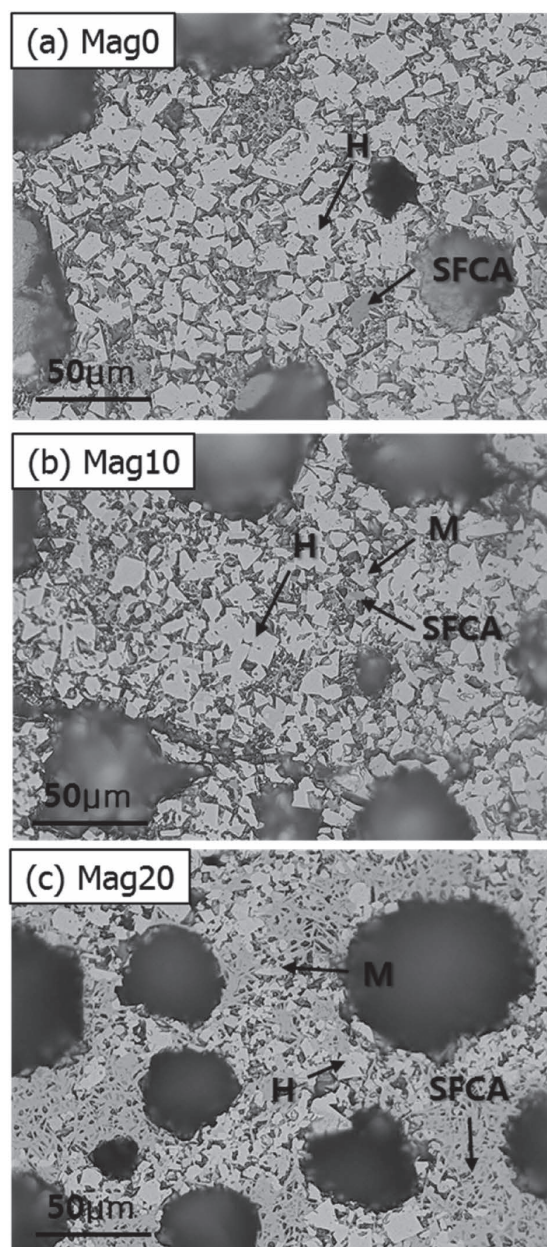


Fig. 4. Optical microscopic observation of the samples (H: hematite, M: magnetite, SFCA: Silico-ferrite of calcium and aluminum).

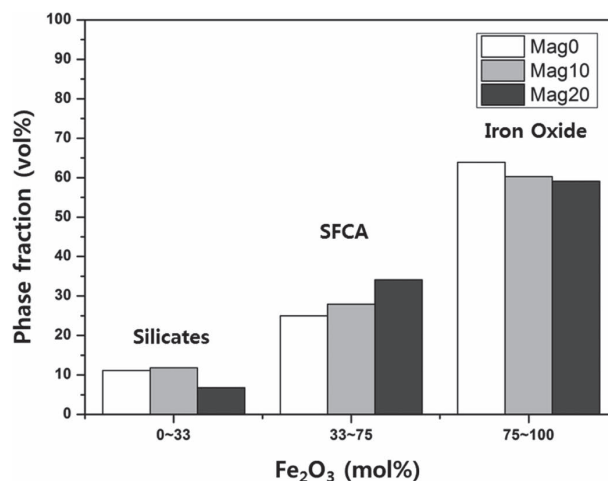


Fig. 5. Phase quantification result from EPMA sweeping area analysis.

observation and phase fraction analysis results, it was found that proper amount of magnetite addition might be effective for promoting the SFCA formation, which decisively affects the sinter quality.

2.4. Compositional Analysis of SFCA Phase

In order to investigate the effect of Fe^{2+} on the SFCA formation, EPMA quantitative analysis was carried out focusing on the SFCA phase. More than 20 points in each sample were analyzed. The distribution of chemical composition of SFCA phase in $\text{CaO-SiO}_2\text{-(Fe}_2\text{O}_3\text{+Al}_2\text{O}_3)$ system is presented in Fig. 6. The plotted SFCA compositions were well fitted to the proposed aenigmatite composition line, $4\text{CaO}\cdot 3\text{SiO}_2$ (C_4S_3)- $\text{CaO}\cdot 3(\text{Fe,Al})_2\text{O}_3$ (CF_3). In addition, it was found that the composition of SFCA tends to move toward CF_3 side along the line with increasing magnetite content. Furthermore, since the magnetite can easily form the silicate phase such as fayalite ($2\text{FeO}\cdot\text{SiO}_2$), some amount of SiO_2 might be consumed to form the silicate phase in the samples with magnetite addition (Mag10 and Mag20). The result indicates that the addition of magnetite reduces the CaO requirement for SFCA formation. That is, more SFCA can be formed with less CaO because Fe^{2+} can directly replace the role of Ca^{2+} as reported by Pownceby and Patrick's study¹⁶⁾ on the substitution mechanism of SFC (Silico-Ferrite of Calcium). In summary, the proper amount of Fe^{2+} originated from magnetite addition in sinter mixture might be effective for producing more SFCA phase with fixed amount of CaO, which results in the improvement of the sinter qualities.

3. Effect of Magnetite Addition on Assimilation Behavior of Quasi-particle using Actual Iron Ores

3.1. Materials Preparation and Experimental Procedure

Since typical magnetite concentrates are very fine in particle size, it can be employed as a constituent of adhering fines in quasi-particle structure. As a case study to examine the effect of magnetite addition on assimilation behavior of quasi-particle, the experiments were carried out using cou-

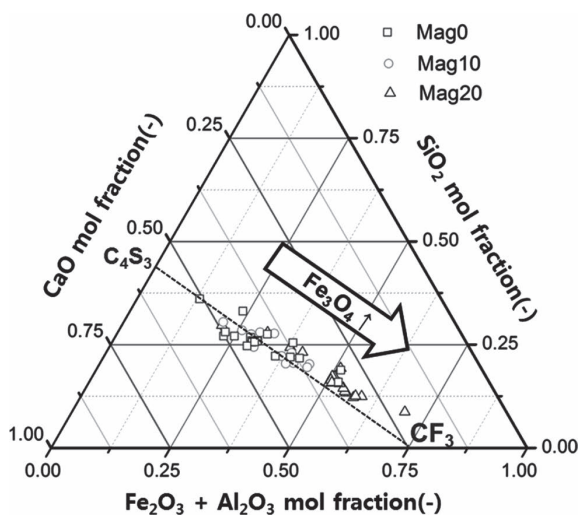


Fig. 6. Distribution of chemical compositions of SFCA phase in $(\text{Fe}_2\text{O}_3\text{+Al}_2\text{O}_3)\text{-SiO}_2\text{-CaO}$ system.

pled ore tablets to simulate quasi-particle structure as shown in Fig. 7. Ore tablet simulating nucleus of quasi-particle ($\Phi 20\text{-}4$ mmh) was prepared with hematite ore C while ore tablet simulating adhering fines of quasi-particle ($\Phi 8\text{-}2.5$ mmh) was prepared with the mixtures of ultra-fine hematite ore N and ultra-fine magnetite ore J (magnetite concentrate). On the basis of ore N, 0 to 100 mass% of ore J were mixed. The samples were named according to the mixing ratio of ore N and ore J; for example, the sample comprising 90 mass% of ore N and 10 mass% of ore J was named N90-J10. In addition, analytical grade of CaCO_3 was mixed as a flux to have the mass ratio of $\text{CaO/Ore}=0.2$ in the ore tablet simulating adhering fines. All the ores were sieved to under $100\ \mu\text{m}$ particle size before pressing the tablet with 10 MPa using hydraulic press. The chemical compositions of used iron ores and prepared ore tablet samples simulating adhering fines of quasi-particle were presented in Tables 2 and 3, respectively. The slight difference in Al_2O_3 (about 0.1 mass%) and SiO_2 (about 0.2 mass%) for the samples between N100-J0 and N70-J30 were ignored and only the change of magnetite content was considered in the subsequent analyses.

As explained above, the assimilation behavior of quasi-particle is a very critical factor determining the final sinter quality. To examine the effect of magnetite addition on assimilation behavior of quasi-particle, a melt penetration test was carried out.^{17,18)} The schematic drawings of sample configuration before and after experiment were shown in

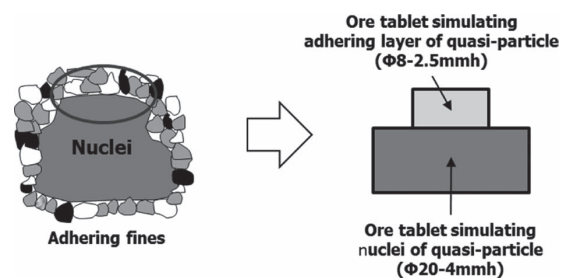


Fig. 7. Coupled ore tablets simulating quasi-particle structure.

Table 2. Chemical compositions of iron ores used in the present study (mass%).

Iron Ore	Total Fe	FeO	Al_2O_3	SiO_2	CaO	Phase
Nuclei Ore C	64.71	0.69	1.35	2.10	0.021	Hematite
Adhering fines Ore N	68.07	0.64	0.47	1.07	0.021	Hematite
Ore J	68.53	27.07	0.043	1.77	0.091	Magnetite

Table 3. Chemical compositions of prepared tablets simulating adhering fines of quasi-particle (mass%).

Sample	Mixing ratio		T.Fe	FeO	Al_2O_3	SiO_2	CaO
	Ore N	Ore J					
N100-J0	100	0	56.73	0.53	0.39	0.89	16.69
N90-J10	90	10	56.77	2.73	0.36	0.95	16.70
N80-J20	80	20	56.80	4.94	0.32	1.01	16.71
N70-J30	70	30	56.84	7.14	0.28	1.07	16.71
N0-J100	0	100	57.11	22.56	0.04	1.48	16.76

Fig. 8. For the melt penetration test, a vertical electrical resistance furnace equipped with automated loading system was employed to simulate the sintering condition. The coupled ore tablets were sintered by changing the sample position inside the furnace whose temperature maintained at 1300°C. The samples were pre-heated at 1100°C for 20 min, and then shifted to the zone of 1300°C for 3 and 7 min, respectively. Subsequently, the sample was withdrawn from the furnace for cooling. Ar atmosphere was maintained during heating and cooling to prevent the oxidation of magnetite. After experiment, a cross-section of sample was analyzed to determine the spread length and penetration depth of melt which are closely related to the assimilation behavior of quasi-particle. They were measured based on the initial interface of coupled ore tablets in terms of an interval between the edges of melted area and an interval from the initial interface to the deepest position of penetrated melt, respectively.

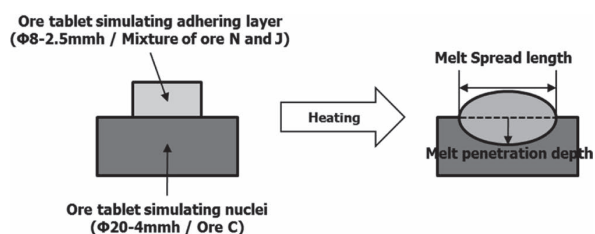


Fig. 8. Schematic drawing of sample configuration before and after experiment.

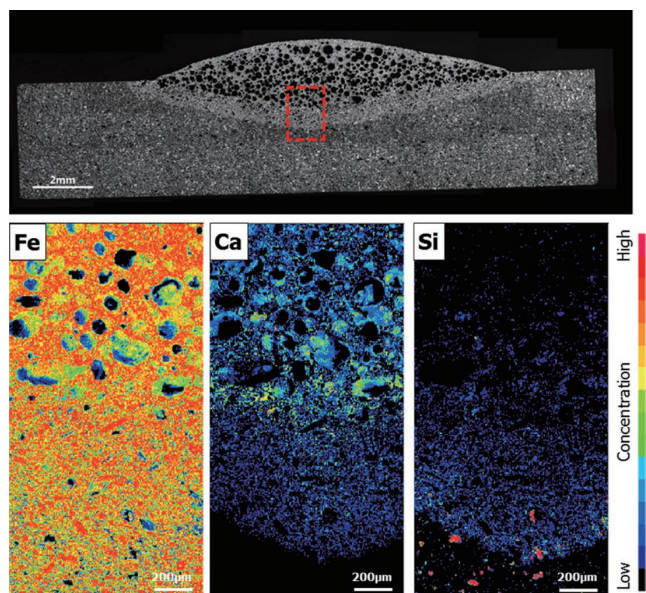


Fig. 9. Cross-section of the coupled ore tablets after melt penetration test and element distribution maps of Fe, Ca and Si.

3.2. Analysis on Melt Penetration Behavior

The cross-section of the coupled ore tablets was analyzed using an optical microscope and EPMA area mapping method as shown in **Fig. 9**. It was clearly shown that the calcium ferrite (SFCA) melt was initiated from the upper ore tablet which simulates the adhering fines and penetrated into the lower ore tablet which simulates the nuclei of quasi-particle structure. The distribution of Ca in the EPMA mapping indicates the depth of melt penetration. **Figure 10** shows the microstructures of the sample penetrated by melt, which can be divided to three domains: melted, interfacial and relict areas. A remarkable difference in pore formation behavior was found in between the melted and interfacial areas. In the melted area, large spherical pores were devel-

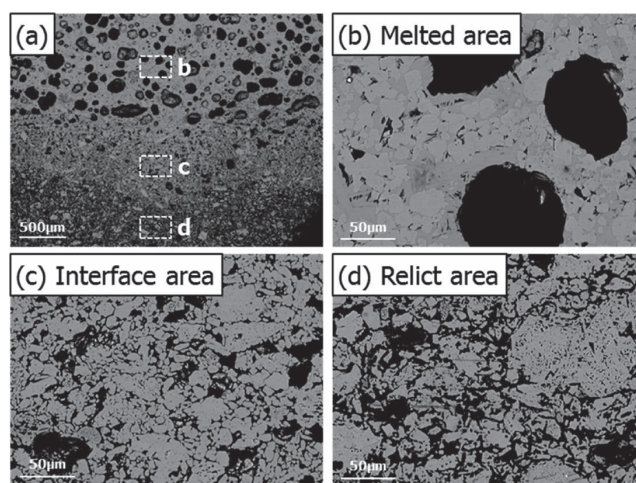


Fig. 10. Microstructure of melt penetrated sample. (b) melted area (c) interface area (d) relict area.

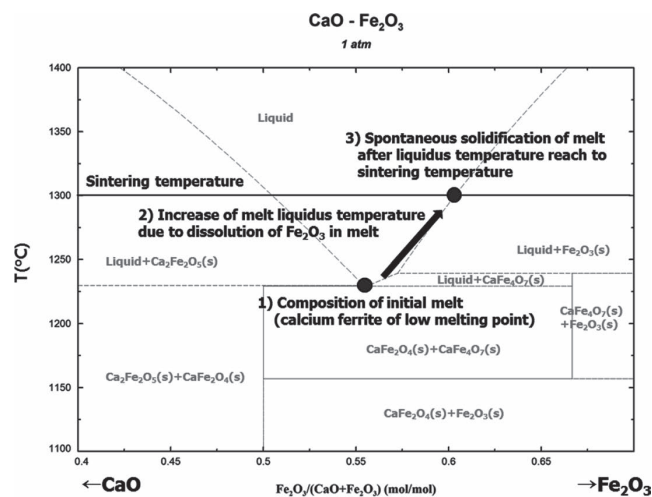


Fig. 11. Sequences of spontaneous solidification of preceding melt.

Table 4. Spread length and penetration depth of melt in the samples.

Holding time	(mm)	N100-J0	N90-J10	N80-J20	N70-J30	N0-J100
3 min	Melt spread length	12.15	14.87	13.95	13.64	10.15
	Melt penetration depth	1.48	1.97	1.95	1.70	1.48
7 min	Melt spread length	11.79	15.11	13.67	12.13	10.33
	Melt penetration depth	1.89	2.18	1.98	1.84	1.54

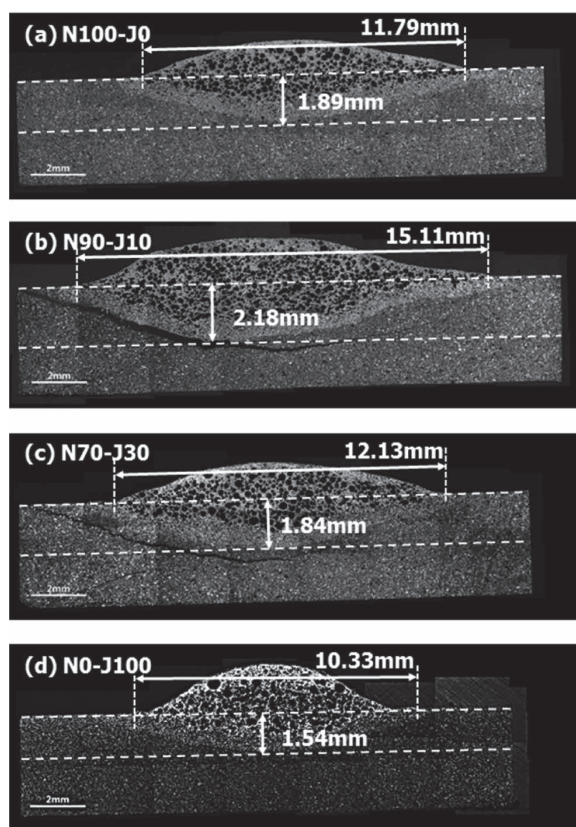
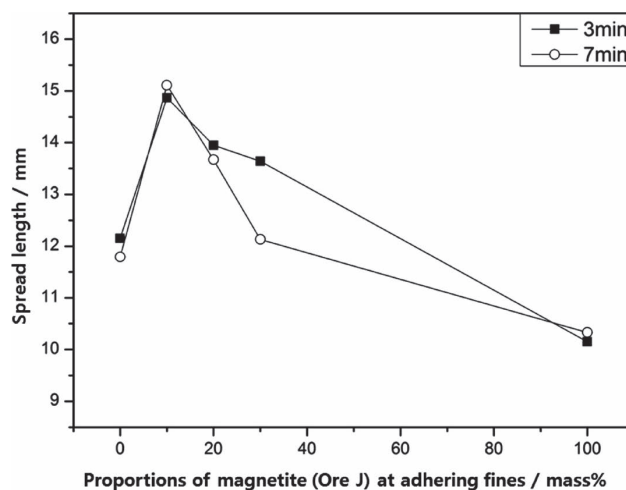


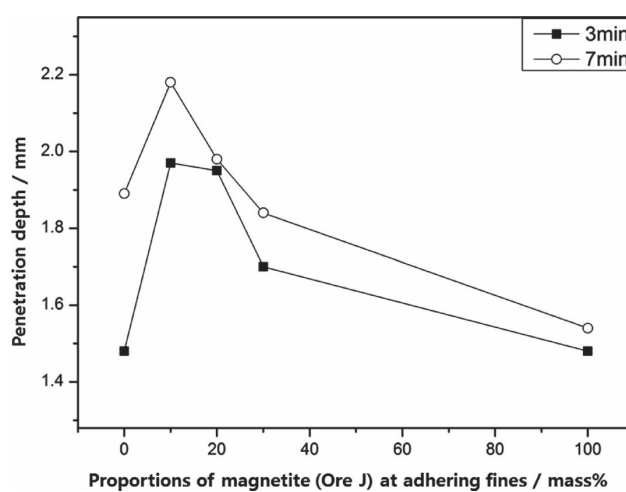
Fig. 12. Example of melt spread length and melt penetration depth measurement for the samples with 7 min holding time.

oped because the calcium ferrite melt with high mobility was solidified during cooling, which results in the development of large pores by pore coalescence. On the other hand, very fine and irregular pores were found in the interfacial area because the high viscous melt was probably solidified during penetration. Since the composition of initiated melt was supposed to be around the calcium ferrite of low melting point and the liquidus temperature of melt was raised by the dissolution of Fe_2O_3 during penetration as shown in the Fig. 11, the viscosity of initial melt was probably increased, resulting in spontaneous solidification without the development of large pores.

The spread length and penetration depth of melts were measured as shown in Fig. 12, and the results were summarized in Table 4. In addition, they were plotted in Fig. 13 along the proportions of magnetite ore J in adhering fines tablet, respectively. The penetration depth of melt sharply increased with adding small amount of magnetite and the highest peak was shown in N90-J10 sample containing 10 mass% magnetite ore J (except CaO content). Then the penetration depth of melt gradually decreased with adding more magnetite ore J. The similar trend with the penetration depth of melt was found in the case of the melt spread length. There was a remarkable difference in between the penetration depth and spread length of melts. That is, the spread lengths of melts held for difference holding time were almost identical while the melt with longer holding time penetrated more deeply. The difference implies that the melt spread length was independent of the holding time. That is, the spread length was maintained once the melt was formed. Therefore, the melt spread length was expected to



(a)



(b)

Fig. 13. Melt spread length (a) and melt penetration depth (b) along the proportions of magnetite ore J in adhering fines tablet.

be determined by the initial melt properties. This indicates that the magnetite addition probably affects the properties of initial melt, which influences the melt penetration depth as well. Since the melt penetration depth was closely related to the assimilation behavior, the proper amount of magnetite addition in adhering fines might be beneficial for the improvement of assimilation behavior of quasi-particle.

3.3. Phase Formation and Initiation Behavior of Melt at Adhering Fines

To correlate the assimilation behavior with phase formation characteristics in adhering fines, the ore tablet simulating adhering fines of quasi-particle was separately heated to 1250°C using image furnace at the heating rate of 2°C/s in an Ar atmosphere. After holding for 10 s at 1250°C, it was quenched by turning off the furnace. Then, after grinding the sample, the X-ray diffraction (XRD) analysis was conducted with Cu $K\alpha$ beam of 40 kV and 40 mA in the 2 theta range of 20 to 80°. Due to the extremely complex nature of calcium ferrites (more specifically SFCA), the exact phase identification was not available. Only the phase formation behavior was qualitatively traced.

As shown in Fig. 14, based on the reference patterns available in the PDF (powder diffraction file) database,

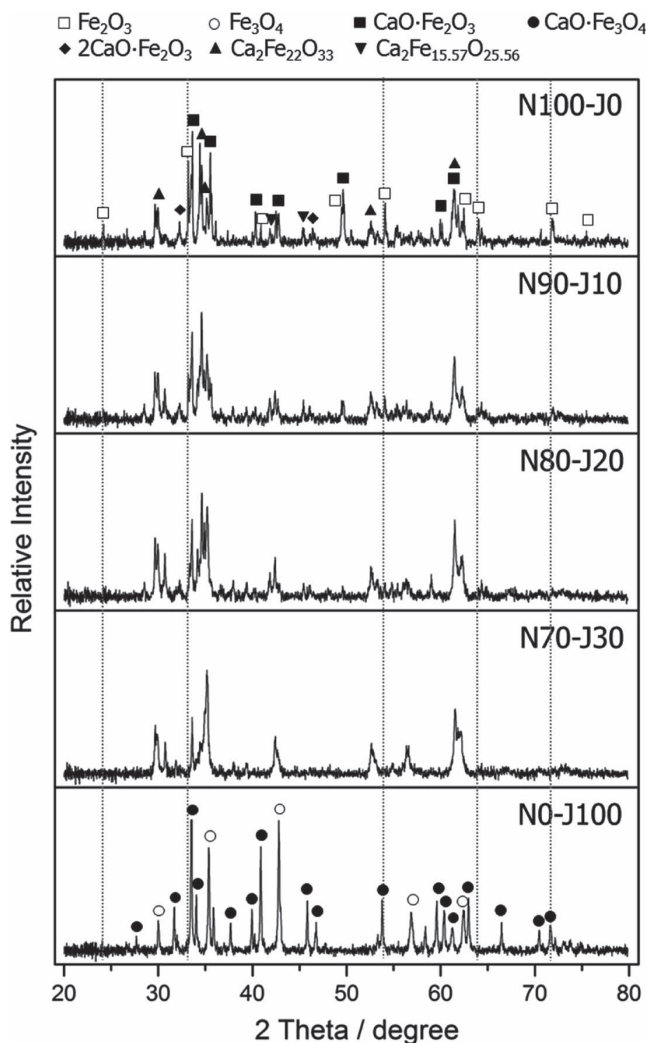


Fig. 14. X-ray powder diffraction result for ore tablet simulating adhering fines of quasi-particle. Some representative phases were marked. The dotted lines indicate main peaks of Fe₂O₃.

some representative phases - Fe₂O₃ (PDF No. 00-033-0664), Fe₃O₄ (PDF No. 01-089-0688), CaFe₂O₄ (PDF No. 00-032-0168), Ca₂Fe₂O₅ (PDF No. 01-071-2264), Ca₂Fe₂₂O₃₃ (PDF No. 00-043-0051), Ca₂Fe_{15.57}O_{25.56} (PDF No. 01-072-2346)-were identified.¹⁹⁾ In the case of N100-J0 sample, mainly Fe₂O₃ and CaO·Fe₂O₃ were identified with some amount of complex calcium ferrite phases such as Ca₂Fe₂₂O₃₃ and Ca₂Fe_{25.57}O_{25.56} which comprised small amount of CaO and large amount of iron oxides. In the samples of N90-J10, N80-J20 and N70-J30, the proportion of Fe₂O₃ was decreased with increasing the amount of magnetite addition, which resulted in higher peaks of calcium ferrite phases. On the other hand, in the case of N0-J100 sample, the phase formation behavior was completely different for the other samples, that is, Fe₃O₄ and CaO·Fe₃O₄ were mainly identified without any complex calcium ferrite phase. This result indicates that the addition of magnetite may alter the calcium ferrite formation reaction which results in increase of calcium ferrite formation.

In addition, melt initiation temperature at adhering fines was determined using DSC (Differential scanning calorimeter) analysis at the heating rate of 10°C/min in an Ar atmosphere. For the analysis, 100 mg of each sample mixture

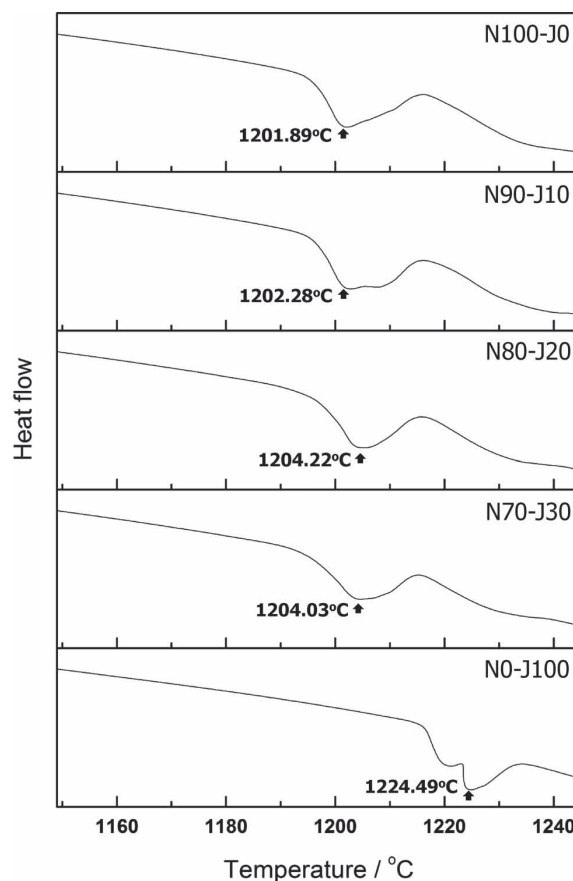


Fig. 15. Differential scanning calorimeter results indicating melt initiation temperature at ore tablet simulating adhering fines.

was used. Figure 15 shows the change of melt initiation temperature with increasing the magnetite content in the sample mixture. The melt initiation temperature was slightly increased with adding magnetite for the samples of N100-J0 to N70-J30 while there was larger variation in melt initiation temperature for the sample of N0-J100. That is, the samples (N90-J10, N80-J20 and N70-J30) containing small amount of magnetite showed similar melt initiation behavior to the sample without magnetite addition, N100-J0. This result may be the evidence which support that added magnetite was participated in the reaction between CaO and Fe₂O₃ to form the calcium ferrite phases.

3.4. Correlation of SFCA Structure and Assimilation Behavior

As mentioned previously, the SFCA (Silico-Ferrite of Calcium and Aluminum) is ‘impure’ calcium ferrite solid solutions with some substitutions of Al₂O₃ and SiO₂ and a substitution mechanism of SFCA can be described as follows:



This work was initially motivated from the presence of Fe²⁺ in the above substitution mechanism and then magnetite was used as a source of Fe²⁺ ions. The analysis results on phase formation and melt initiation temperature at the adhering fines showed that the added magnetite directly participated in the SFCA formation reaction, resulting in remarkable structural variation of SFCA. In addition, the

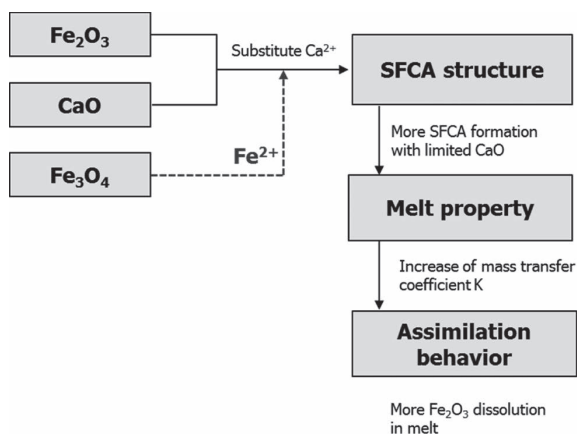


Fig. 16. The proposed mechanism interpreting how magnetite addition affects the assimilation behavior of quasi-particle.

structural variation of SFCA at adhering fines changed the properties of initial melt causing the variations in the spread length and penetration depth of melts. On the basis of these experimental results, the dissolution of Fe_2O_3 from nuclei to melt during assimilation of quasi-particle was interpreted as follows:¹⁰⁾

$$\frac{dm}{dt} = K \cdot A_r \cdot \Delta c^n \dots\dots\dots (3)$$

where m represents the mass of dissolved solid, t is reaction time, K is a proportionality constant, A_r is the area normal to the direction of mass transfer, Δc is the concentration driving force, and n is a constant. The value K is dependent on the assimilation mechanism. It is the reaction rate constant if the assimilation is controlled by dissolution reaction while it is the mass transfer coefficient if the assimilation is mass transfer controlled. The driving force is the concentration difference of Fe_2O_3 in between the nucleus and melt. The constant n is 1 when mass transfer is the rate-controlling step while it is greater than 1 when dissolution reaction is important. The assimilation will be terminated when melt composition reach the saturation value (*i.e.* the liquidus temperature of melt at sintering temperature). Loo and Matthews¹⁰⁾ found that the assimilation took place by mass transfer control, then the value K should be the mass transfer coefficient and the constant n was 1.

Since added magnetite (more specifically Fe^{2+} in magnetite) influences the SFCA structure by directly substituting Fe^{2+} for Ca^{2+} ,¹⁴⁾ more SFCA can be formed with fixed amount of CaO . Then more Fe_2O_3 can be dissolved into melt by increasing the mass transfer coefficient, K under some assumptions that the reaction area and concentration difference are constant. From the structural viewpoint of the above substitution mechanism, the role of Fe^{2+} in SFCA is that it directly replaces Ca^{2+} and probably controls the capability of Fe_2O_3 dissolution into SFCA. The proposed mechanism for interpreting how magnetite addition affects the assimilation behavior of quasi-particle was summarized in Fig. 16. Although the mechanism is still not clear yet, the above experimental results might provide clear evidence that small amount of magnetite addition to adhering fines could have significant influence on the melt properties or

SFCA structure as well as the assimilation behavior of quasi-particle.

4. Conclusions

In the present study, the magnetite concentrate was utilized as an additive to adhering fines of quasi-particle and the effect of magnetite addition on assimilation behavior was investigated. From the findings, the following conclusions were obtained.

(1) In a basic study on melting and phase formation behavior, small amount of magnetite addition, more specifically Fe^{2+} in magnetite, was found to significantly affect the physicochemical properties of melt as well as the final sinter microstructure. More SFCA was formed with fixed CaO because Fe^{2+} directly replaces Ca^{2+} in the substitution mechanism of SFCA.

(2) In a case study on the assimilation behavior, the added magnetite was found to affect the SFCA structure by substituting Fe^{2+} for Ca^{2+} and control the capability of Fe_2O_3 dissolution in SFCA. With proper amount of magnetite addition, more Fe_2O_3 can dissolve into melt which results in the improvement of assimilation behavior of quasi-particle.

(3) Although the exact mechanism is still not clearly clarified, the current work might provide clear experimental evidence that proper amount of magnetite addition to adhering fines can improve the assimilation behavior of quasi-particle.

Acknowledgement

The authors would like to gratefully acknowledge Prof. Yasushi Sasaki for his invaluable advise and discussions.

REFERENCES

- 1) K. Inoue and T. Ikeda: *Tetsu-to-Hagané*, **68** (1982), 2190.
- 2) W. G. Mumme: *N. Jb. Miner. Mh.*, **8** (1988), 359.
- 3) E. Da Costa and J. P. Coheur: *Ironmaking Steelmaking*, **22** (1995), 223.
- 4) M. I. Pownceby and T. R. C. Patrick: *Eur. J. Mineral.*, **12** (2000), 455.
- 5) T. R. C. Patrick and M. I. Pownceby: *Metall. Mater. Trans. B*, **33B** (2002), 79.
- 6) S. W. Kim, Y. K. Ji and I. K. Suh: *POSCO Res. paper*, **18** (2013), 1.
- 7) N. Oyama, H. Sato, K. Takeda, T. Ariyama, S. Masumoto, T. Jinno and N. Fuji: *ISIJ Int.*, **45** (2005), 817.
- 8) N. Oyama, T. Higuchi, S. Machida, H. Sato and K. Takeda: *ISIJ Int.*, **49** (2009), 650.
- 9) D. Debrincat, C. E. Loo and M. F. Hutchens: *ISIJ Int.*, **44** (2004), 1308.
- 10) C. E. Loo and L. T. Matthews: *Trans. Inst. Min. Metall. C*, **101** (1992), 105.
- 11) C. E. Loo and W. Leung: *ISIJ Int.*, **43** (2003), 1393.
- 12) L. X. Yang: *ISIJ Int.*, **45** (2005), 469.
- 13) J. M. F. Clout and J. R. Manuel: *Powder Technol.*, **130** (2003), 393.
- 14) Z. Wang, K. Ishii, Y. Sasaki, T. Tsutsumi, K. Higuchi and Y. Hosotani: *Tetsu-to-Hagané*, **84** (1998), 689.
- 15) Z. Wang, Y. Sasaki, Y. Kashiwaya and K. Ishii: *Tetsu-to-Hagané*, **86** (2000), 370.
- 16) M. I. Pownceby and T. R. C. Patrick: *Eur. J. Mineral.*, **12** (2000), 455.
- 17) J. Okazaki, K. Higuchi, Y. Hosotani and K. Shinagawa: *ISIJ Int.*, **43** (2003), 1384.
- 18) S. Yoshimura, K. Kurosawa, Y. Gonda, S. Sukenaga, N. Saito and K. Nakashima: *ISIJ Int.*, **49** (2009), 687.
- 19) J.-M. Le Meins, L. M. D. Cranswick and A. Le Bail: *Powder Diffraction*, **18** (2003), 106.